Translational Oncology
www.transonc.com

Volume 11 Number xx Month 2018 pp. 575–584 575

Silencing of Discoidin Domain Receptor-1 (DDR1) Concurrently Inhibits Multiple Steps of Metastasis Cascade in Gastric Cancer[1]

Ryo Yuge[*], Yasuhiko Kitadai[†], Hidehiko Takigawa[‡], Toshikatsu Naito[‡], Naohide Oue[§], Wataru Yasui[§], Shinji Tanaka[*] and Kazuaki Chayama[‡]

[*]Department of Endoscopy, Hiroshima University Hospital, Hiroshima, Japan; [†]Department of Health Sciences, Prefectural University of Hiroshima; [‡]Department of Gastroenterology and Metabolism, Graduate School of Biomedical and Health Sciences, Hiroshima University, Hiroshima, Japan; [§]Department of Molecular Pathology, Graduate School of Biomedical and Health Sciences, Hiroshima University, Hiroshima, Japan

Abstract

Accumulating evidence suggests that a unique set of receptor tyrosine kinases, known as discoidin domain receptors (DDRs), plays a role in cancer progression by interacting with the surrounding collagen matrix. In this study, we investigated the expression and role of DDR1 in human gastric cancer metastasis. Proliferation, migration, invasion, and tube formation assays were conducted in DDR1-expressing MKN74 gastric cancer cells and corresponding DDR1-silenced cells. The effects of DDR1 on tumor growth and metastasis were examined in orthotopically implanted and experimental liver metastasis models in nude mice. The expression of DDR1 in surgical specimens was analyzed by immunohistochemistry. DDR1 was expressed in human gastric cancer cell lines, and its expression in human gastric tumors was associated with poor prognosis. Among seven gastric cancer cell lines, MKN74 expressed the highest levels of DDR1. DDR1-silenced MKN74 cells showed unaltered proliferation activity. In contrast, migration, invasion, and tube formation were significantly reduced. When examined in an orthotopic nude mouse model, DDR1-silenced implanted tumors significantly reduced angiogenesis and lymphangiogenesis, thereby leading to reductions in lymph node metastasis and liver metastasis. In a model of experimental liver metastasis, DDR1-silenced cells almost completely inhibited liver colonization and metastasis. DDR1 deficiency led to reduced expression of the genes encoding vascular endothelial growth factor (VEGF)-A, VEGF-C, and platelet-derived growth factor-B. These results suggest that DDR1 is involved in gastric cancer tumor progression and that silencing of DDR1 inhibits multiple steps of the gastric cancer metastasis process.

Translational Oncology (2018) 11, 575–584

Introduction

Gastric cancer (GC) is the fourth most common type of cancer and the second leading cause of cancer-associated mortality worldwide [1]. Although numerous novel chemotherapy regimens have been developed and surgical skills and instruments for the treatment of GC have also improved, the survival rate remains low [2]. One of the reasons for the poor prognosis of GC is the inability of anticancer agents to target tumor cells and tissues selectively [3]. Thus, the search for a promising therapeutic target and a novel prognostic biomarker

Address all correspondence to: Yasuhiko Kitadai, MD, PhD, Department of Health Sciences, Prefectural University of Hiroshima, 1-1-71 Ujinahigashi, Minami-ku, Hiroshima 734-0003, Japan.
E-mail: kitadai@pu-hiroshima.ac.jp

[1] This work was supported, in part, by Grants-in-Aid for Cancer Research from the Ministry of Education, Culture, Science, Sports and Technology of Japan. The authors have no conflict of interest to report.
Received 6 October 2017; Revised 29 January 2018; Accepted 1 February 2018

1936-5233/17
https://doi.org/10.1016/j.tranon.2018.02.003

for GC is of great interest. GC tissues often show histological heterogeneity, containing intestinal and diffuse subtypes. In particular, the diffuse type of GC has rich stromal components, consisting of rich collagen [4]. Recently, the interaction between cancer cells and the stroma has been thought to be primarily responsible for tumor progression and metastasis.

Discoidin domain receptors (DDRs) are unique receptor tyrosine kinases (RTKs) that bind to and are activated by collagens [5,6]. Among the collagen receptor families, DDRs are the only RTKs phosphorylated by various collagens [7–9]. Various types of collagen act as ligands for DDRs. DDR1 is activated by collagens of type I-VI and VIII, whereas DDR2 is activated by the fibrillar collagens, in particular the collagens of type I and type III [7]. DDR1 is reported to be preferentially expressed in highly invasive cancer cells, whereas DDR2 is mainly expressed in surrounding stromal cells [10].

DDR1 has been reported to be highly expressed in a variety of neoplasms, including those in the lung, liver, ovary, and breast, and other types of tumors [11–14]. In highly invasive non–small cell lung cancer, DDR1 is reported to be significantly correlated with lymph node metastasis and poor prognosis [11,15]. In pancreatic ductal adenocarcinoma, high expression of DDR1 was found to be significantly associated with poor prognosis [16]. Recently, Hoon et al. reported that DDR1 expression in GC patients receiving adjuvant chemotherapy was an independent prognostic factor [17]. DDR1 is reported to regulate diverse functions of tumor cells, including cellular adhesion and morphogenesis, differentiation, migration and invasion, extracellular matrix (ECM) remodeling, proliferation, and apoptosis [14,18–20]. However, the role of DDR1 in GC progression and metastasis is not yet well understood.

Thus, we analyzed the function of DDR1 using DDR1 shRNA. In addition, we investigated the expression of DDR1 using immunohistochemistry to clarify its clinicopathological significance in human GC tissues.

Materials and Methods

Surgical Specimens of GC Tissues

Primary tumors were collected from patients diagnosed with GC and treated at the Hiroshima University Hospital. For immunohistochemical analysis, we used archival formalin-fixed, paraffin-embedded tumor samples from 127 patients who underwent surgical resection for GC. Histological classification (intestinal, diffuse-adherent, and diffuse-scattered types) was performed according to the Lauren classification system [21,22]. Tumor staging was performed according to the TNM classification system. Patient privacy was protected in accordance with the Ethical Guidelines for Human Genome/Gene Research of the Japanese Government.

Human GC Cell Lines and Culture Conditions

This study examined seven human GC cell lines. MKN1, MKN45, MKN74, HSC39, and KATO-III were purchased from the Japanese Collection of Research Bioresources Cell Bank (Osaka, Japan). TMK1 was kindly gifted by Dr. W. Yasui (University of Hiroshima, Japan). KKLS was kindly gifted by Dr. Takahashi (University of Kanazawa, Japan). These cell lines were maintained in Dulbecco's modified Eagle's medium with 10% fetal bovine serum (FBS; Sigma-Aldrich, St. Louis, MO) and a penicillin-streptomycin mixture. The cultures were maintained for no longer than 12 weeks after the recovery of cells from frozen stock.

Immunohistochemistry

Immunohistochemical staining of paraffin-embedded tissue sections was conducted. The procedures for immunohistochemical detection were as described previously [23]. Primary antibodies were as follows: polyclonal rabbit anti-DDR1 (Abcam, Cambridge, UK); Ki-67 equivalent antibody (Novocastra; Leica Microsystems, Newcastle upon Tyne, UK); polyclonal rabbit anti-mouse type I collagen (Novotec, Saint-Martin-La-Garenne, France); polyclonal rabbit anti-CD31 (Abcam); polyclonal rat anti-Lyve1 (R&D Systems, Minneapolis, MN); polyclonal rabbit anti phospho-DDR1 (Cell Signaling Technology, Danvers, MA); polyclonal rabbit anti-GFP (Novus Biologicals, Littleton, CO). Transplanted tumor tissues were prepared into 10-mm frozen sections and then were subjected to immunofluorescence analyses using the following primary antibodies: CD31, Lyve-1, type I collagen, p-DDR1, and GFP. The fluorescent signal of secondary antibody was captured by confocal laser-scanning microscopy (Carl Zeiss Microscopy, Jena, Germany). DDR1 staining was considered positive if at least 30% of the cancer cells were stained.

DDR1 Silencing

For DDR1 silencing, lentiviral particles for shRNA knockdown were purchased from Santa Cruz Biotechnology (Dallas, TX), including Control Lentiviral Particles (#sc-108080) and DDR1 shRNA(h) Lentiviral Particles (#sc-35187-v). MKN74 cells were transfected with shDDR1 and scrambled shRNA lentiviral particles according to the manufacturer's instructions. Forty-eight hours postinfection, cell populations were incubated in medium containing the appropriate antibiotic (puromycin) for 2 additional weeks. Antibiotic-resistant pools were expanded and frozen at each cell passage.

Western Blot Analysis and Immunoprecipitation

Cultured GC cells were washed and then scraped into phosphate-buffered saline containing 5 mmol/L EDTA and 1 mmol/l sodium orthovanadate. Pellets obtained by centrifugation were resuspended in a lysis buffer (20 mmol/l Tris-HCl, pH 8.0; 137 mmol/l NaCl; 10% glycerol; 2 mmol/l EDTA; 1 mmol/l phenylmethylsulfonyl fluoride; 20 mmol/l leupeptin; 0.15 U/ml aprotinin) and centrifuged. The supernatant was then collected. Protein lysates from each sample were resolved by sodium dodecyl sulfate polyacrylamide gel electrophoresis followed by blotting using anti-DDR1 (#sc-532, Santa Cruz Biotechnology) or anti–β-actin (Sigma-Aldrich) and detection using an enhanced chemiluminescence system.

To assess collagen-induced DDR1 phosphorylation, cell growth was arrested by incubation in serum-free medium for 16 hours and then stimulated with collagen I at 15 μg/ml. For immunoprecipitation assay, 500 μg cell lysate was mixed with rabbit anti-DDR1 antibody (Santa Cruz Biotechnology) overnight at 4°C, and then 40 μl protein-A beads (Cell Signaling Technology) was added and mixed for 1 hour. The protein-bead complexes were washed three times with lysis buffer and subjected to sodium dodecyl sulfate polyacrylamide gel electrophoresis. This was followed by blotting using anti-phosphotyrosine antibodies (4G10; Upstate Biotechnology, Charlottesville, VA) and detection using an enhanced chemiluminescence system.

Quantitative Reverse Transcription Polymerase Chain Reaction (qRT-PCR)

Total RNA was extracted from GC cell lines with an RNeasy Kit (Qiagen, Tokyo, Japan) according to the manufacturer's instructions. cDNA was generated from 1 μg total RNA with a first-strand cDNA

synthesis kit (Amersham Biosciences, Buckinghamshire, UK); 1 μl of cDNA was amplified with SYBR-Green in 20-μl reactions, as previously described [24]. The primer sequences used in this study are summarized in Supplementary Table 1. Expression levels were normalized with GAPDH as an internal control. The experiments were performed in triplicate.

Cellular Proliferation, Migration, and Invasion Assay

Cell proliferation, wound-scratch migration, and invasion assays were conducted using a brightfield image label-free high-content time-lapse assay system (IncuCyte Zoom system; Essen BioScience, Ann Arbor, MI) according to the manufacturer's instructions. In brief, for the proliferation assay, equal numbers of cells (1×10^5/well) were seeded onto type I collagen (Trevigen, Gaithersburg, MD)–coated 12-well plates in the appropriate culture medium with supplements or agents, and the percent cell confluence was then continuously measured using the IncuCyte Zoom system over a 5-day period. For the migration assay, cells (1.2×10^5 cells/well) were seeded onto type I collagen (Trevigen)–coated 96-well ImageLock tissue culture plates (Essen BioScience). Once cells reached >90% confluence, at 12 hours after seeding, wound scratches were made using a 96-pin WoundMaker (Essen BioScience), and relative wound densities were measured using the IncuCyte Zoom system over a 5-day period. For the invasion assay, cells were overlaid with a layer of Matrigel (BD Biosciences, San Diego, CA) after creating the wound scratches and conducting the migration assay. The microplate was then incubated in a 37°C CO_2 incubator for 30 minutes to allow the Matrigel to gel and then was overlaid with complete medium. Relative wound densities were measured using the IncuCyte Zoom system over a 5-day period. The experiments were performed in triplicate.

Tube Formation Assay

For preparation of conditioned medium, MKN74 and DDR1-silenced MKN74 cells were seeded on type I collagen–coated dishes and cultured in fresh medium supplemented with 10% FBS until confluence. Cells were briefly rinsed twice with phosphate-buffered saline followed by incubation with medium supplemented with 1% FBS for 48 hours prior to collection of the culture medium. Cell culture supernatants were centrifuged at 2000 rpm for 10 minutes for removal of cell debris. Human umbilical vein endothelial cells (HUVECs) were incubated in 100-μl conditioned medium in 96-well plates coated with 60 μl Matrigel (BD Biosciences) at a density of 2×10^4 cells per well. After 24 hours, the number of tubes formed by HUVECs was quantified from three randomly chosen fields (10×).

Animals and Orthotopic Implantation of Tumor Cells

Female athymic BALB/c nude mice were obtained from Charles River Japan (Tokyo, Japan). Mice were maintained under specific pathogen-free conditions and used at 8 weeks of age. The study was conducted with permission from the Committee on Animal Experimentation of Hiroshima University. To produce gastric tumors, 1×10^6 cells in 50 μl of Hank's balanced salt solution were injected into the gastric walls of nude mice under zoom stereomicroscope observation (Carl Zeiss, Gottingen, Germany). To produce experimental liver metastasis, 1×10^6 cells in 50 ml of Hanks' balanced salt solution were injected into the spleens of nude mice.

Necropsy and Histological Studies

Mice bearing orthotopic tumors were euthanized with pentobarbital, and body weights were recorded. After necropsy, tumors were excised and weighed. For immunohistochemistry, one part of the tumor tissue was fixed in formalin-free immunohistochemistry zinc fixative (BD Pharmingen, San Diego, CA) and embedded in paraffin; the other part was embedded in Tissue-Tek OCT compound (Sakura Finetek, Torrance, CA), rapidly frozen in liquid nitrogen, and stored at –80°C. All macroscopically enlarged regional (celiac and para-aortal) lymph nodes were harvested, and the presence of metastatic disease was confirmed by histological examination.

Quantification of Microvessel Area and Ki-67 Labeling Index

To evaluate the angiogenic and lymphangiogenic activity of the tumors, the areas of microvessels (CD31+) and lymphatic vessels (Lyve-1+) were quantified. Ten random fields at ×400 magnification were captured for each tumor, and the vessel area including the lumen was calculated with the use of ImageJ software version 1.47v (NIH, Bethesda, MD). The Ki-67 labeling index was determined by light microscopy at the site of the greatest number of Ki-67+ cells. Cells were counted in 10 fields at 200× magnification, and the number of Ki-67+ cells among approximately 300 tumor cells was counted and expressed as a percentage.

Statistical Analysis

Between-group differences in proliferation, migration, invasion, animal experiments, microvessel area, percentage of Ki-67+ cells, and tube number were analyzed by Mann-Whitney *U* tests. Differences in gene expression levels between control cells and DDR1-silenced cells were analyzed by Student's *t* test. The χ^2 test was used to analyze the association between DDR1 and each patient clinicopathological parameter. Kaplan-Meier curves were generated to study the survival rate. $P < .05$ was considered statistically significant. Data are expressed as means ± SEM.

Results

Expression of DDR1 in GC Cell Lines

To evaluate the expression levels of DDR1 in human GC cell lines, qRT-PCR and Western blot analysis were conducted in seven GC cell lines. As shown in Figure 1, *A* and *B*, upregulated DDR1 expression levels were found in several cell lines, with the highest levels in MKN74 cells.

Effects of DDR1 Silencing on Cell Proliferation, Migration, and Invasion

In order to investigate the biological function of DDR1 in GC, we examined the effect of DDR1 silencing using shRNA on cell proliferation activity, migration activity, and invasiveness. MKN74 GC cells, which express the highest levels of DDR1 among seven GC cell lines, were selected for these experiments. MKN74 cells were transfected with shDDR1 and scrambled shRNA lentiviral particles. DDR1 expression levels, as analyzed by qRT-PCR, were downregulated by about 85% in these cells as compared to levels in cells transduced with scrambles shRNA (Figure 1*C*). The qRT-PCR results were validated by Western blot analysis (Figure 1*D*). Under collagen stimulation, phosphorylation of DDR1 was lower in DDR1-silenced MKN74 cells than in MKN74 control cells (Figure 1*E*).

Next, we examined the role of DDR1 in proliferation, migration, and invasion using the IncuCyte Zoom system. We identified no

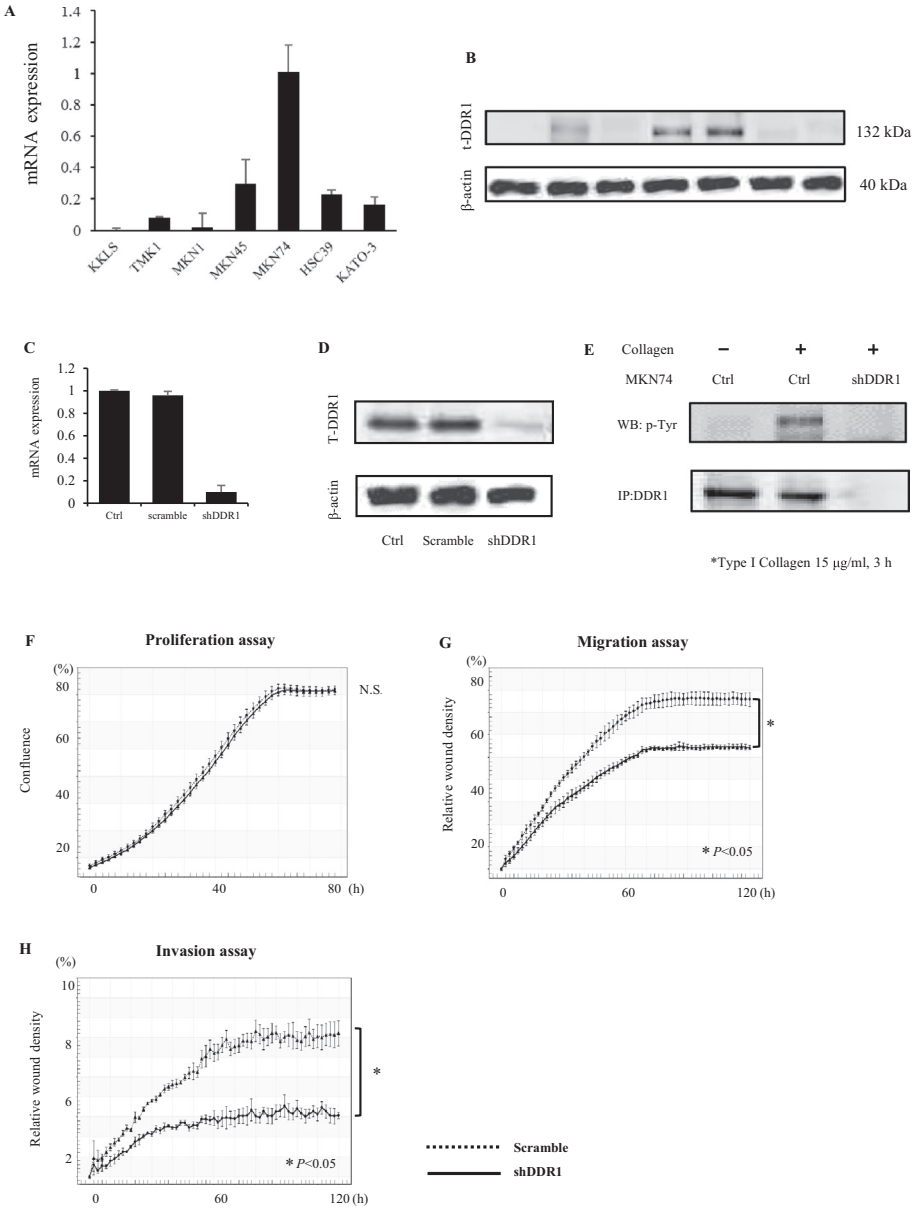

Figure 1. Expression and function of DDR1 in GC. (A-B) Expression of DDR1 in human GC cell lines. Expression levels of DDR1 mRNA in GC cells were quantified by qRT-PCR ($n=3$) (A) and Western blot (B). (C-E) Generation of DDR1 knockdown in MKN74 cells. MKN74 cells were transfected with shDDR1 and scrambled shRNA lentiviral particles. At 48 hours postinfection, cells were selected with puromycin. DDR1 knockdown was confirmed by qRT-PCR ($n=3$) (C) and Western blot analysis (D). (E) Immunoprecipitation (IP) of DDR1 from cell lysates of MKN74 after incubation with or without collagen I (15 μg/ml) for 3 hours. The blots were probed with anti-phosphotyrosine antibody and subsequently reprobed with anti-DDR1. (F-H) Effects of DDR1 knockdown on proliferation, migration, and invasion. (F) No differences were observed in cell proliferation following DDR1 knockdown. (G-H) Cells transduced with DDR1 shRNA exhibited significantly inhibited migration and invasion compared to control cells. All assays were measured using IncuCyte technology, which monitors cell activity in real time (one image every 2 hours) for a period of 3 to 5 days.

significant differences in cell proliferation in DDR1-silenced cells versus control cells (Figure 1*F*). In contrast, migration activity was significantly lower in DDR1-silenced cells as compared with that in control cells in the presence of collagen (Figure 1*G*). Similarly, whereas control MKN74 cells invaded the Matrigel, DDR1-silenced cells were significantly less invasive (Figure 1*H*). These results indicate that DDR1 stimulates cell migration and invasion in GC cells.

DDR1 Silencing Inhibits Metastasis

On the basis of our *in vitro* results, we decided to determine how DDR1 affects the progression of GC using an orthotopically implanted nude mouse model. Both MKN74 control cells and DDR1-silenced cells were implanted into the gastric walls of the nude mice, and mice were sacrificed 6 weeks after implantation (Table 1). Tumor incidence was 100% in both groups. Although there was no significant difference in tumor weight, lymph node metastasis was significantly inhibited in the DDR1-silenced implanted tumors. Liver metastasis was also completely inhibited in DDR1-silenced implanted tumors.

Histopathological Analysis of Orthotopically Implanted Tumors

MKN74 parental cells orthotopically implanted into the gastric walls of nude mice grew invasively with a stromal reaction (Figure 2*A*, *left*). In

Table 1. Results of Animal Experiments (Orthotopic Implanted Tumor)

Group	Tumor incidence	Body weight (g)	Tumor weight (g)	Lymph node metastasis		Liver metastasis
MKN74 scramble (Ctrl) (n=9)	9/9	19.3 (17.0 to 23.0)	0.13 (0.12 to 0.21)	7/9	*	2/9
MKN74 DDR1 shRNA (n=10)	10/10	21.6 (18.2 to 25.0)	0.10 (0.08 to 0.12)	2/10		0/10

*P<.05.

contrast, DDR1-silenced cells grew expansively, and necrosis was observed at the central area of the tumor (Figure 2*A*, *right*). Differences in DDR1 expression in the tumor cells were confirmed by immunohistochemistry. In MKN74 control tumors, DDR1 was observed in the membranes and cytoplasms of cancer cells, whereas there was no DDR1 staining in DDR1-silenced implanted tumors (Figure 2*B*). In control tumors, the expression of pDDR1 was observed, and type I collagen was located around these activated cancer cells (Figure 2*C*, *left*). In DDR1-silenced implanted tumors, activated DDR1 was not expressed by cancer cells (Figure 2*C*, *right*). The

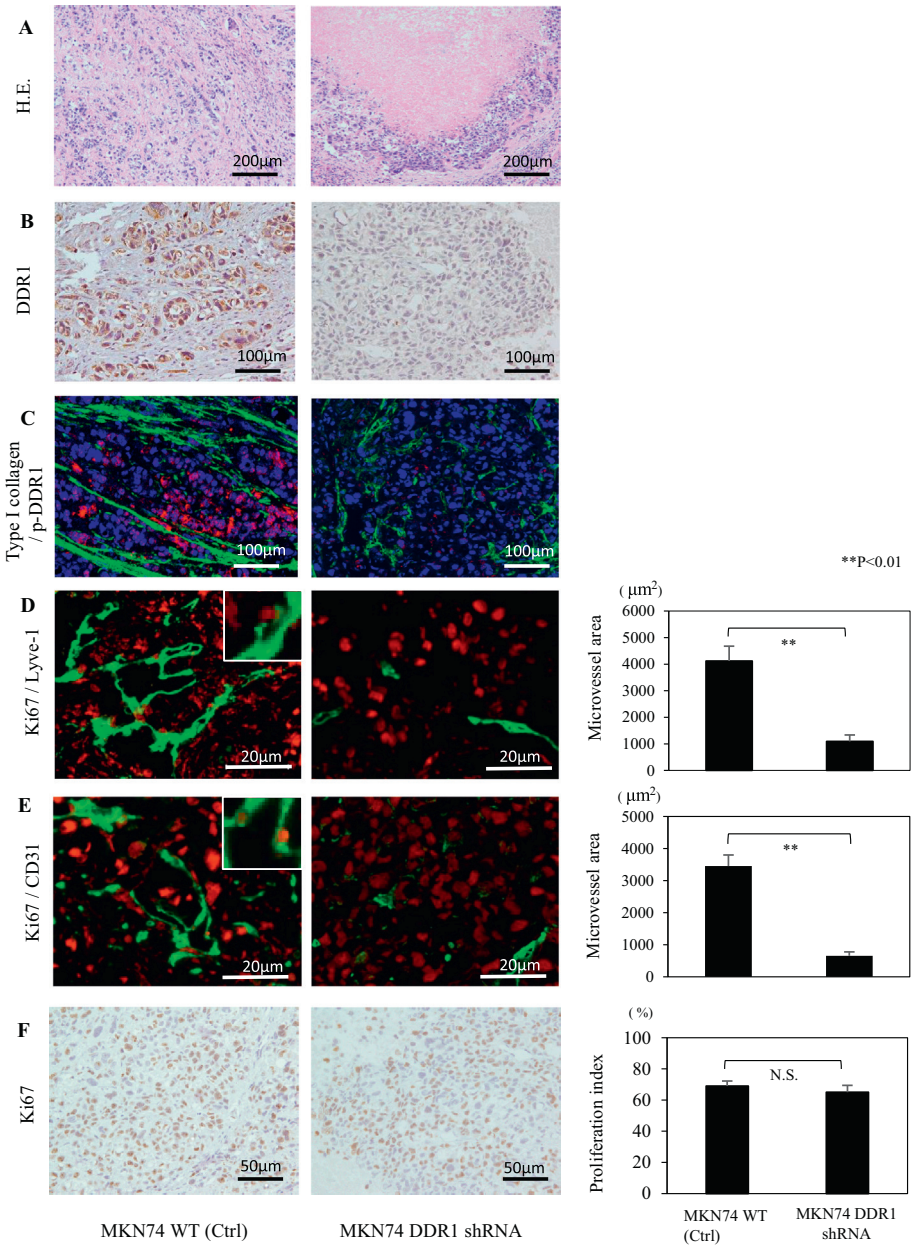

Figure 2. Effect of DDR1 silencing on MKN74 orthotopically implanted tumor growth. Histological and immunofluorescent staining of orthotopic tumors at 28 days after cell implantation. (A) Hematoxylin and eosin staining. DDR1-silenced implanted tumors grew expansively, and necrosis was observed at the tumor center (right). (B) DDR1 expression was attenuated in tumors transfected with DDR1 shRNA (right). (C) In control tumors, there were rich collagen bands, and phosphorylated DDR1 was detected in cancer cells (left). Type I collagen: green, p-DDR1: red, DAPI: blue. (D, E) Mean densities of lymphatic and blood vessels were significantly reduced in DDR1-silenced tumors. The insets show high-magnification images of Ki-67 signal detected in the vessels of control tumors. There was no Ki-67 signal detected in the vessels of DDR1-silenced tumors. Ki-67: red, Lyve1 and CD31: green. (F) Analysis of cell proliferation (Ki-67). There was no significant difference in the Ki-67 proliferation indexes. Data are expressed as means ± SEM. **P < .01.

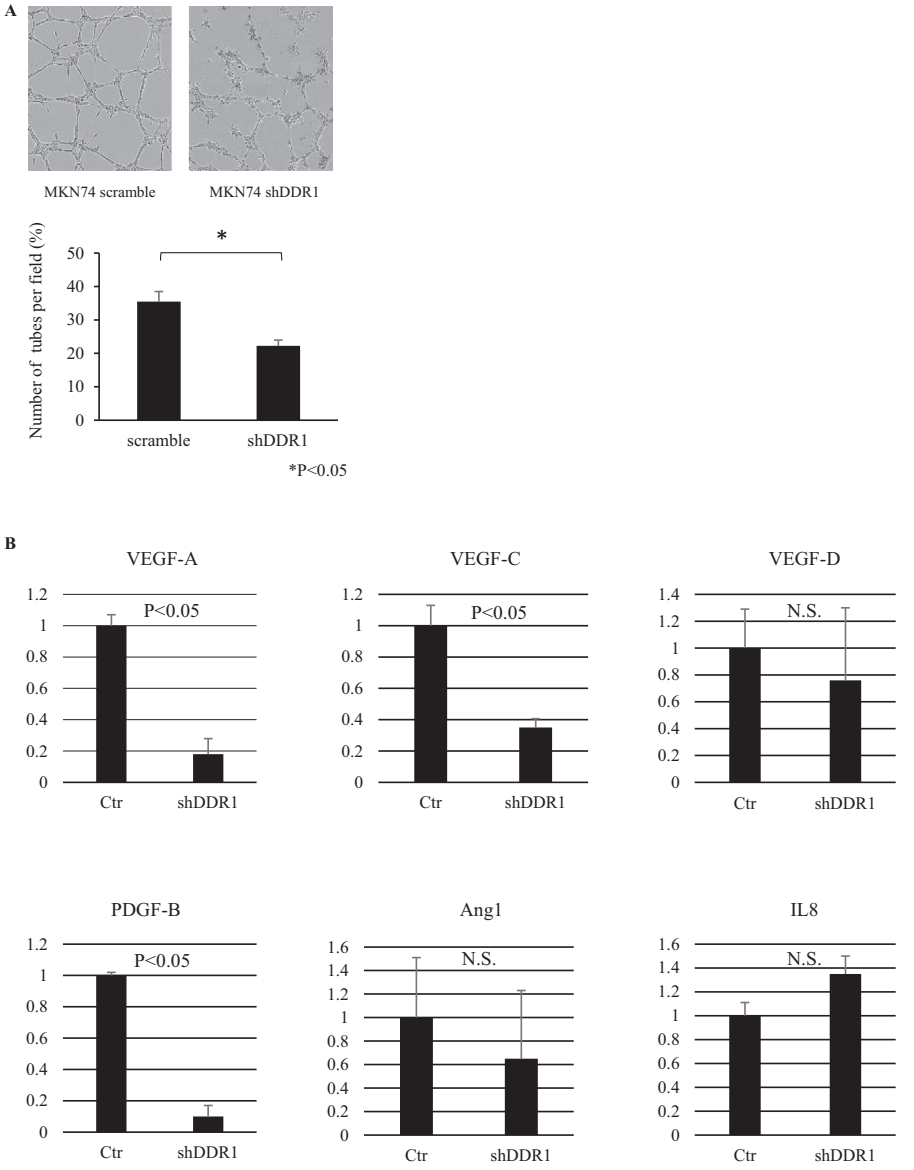

Figure 3. Effects of DDR1 silencing on angiogenesis. (A) Tube formation assay. The mean number of complete tubular structures formed by HUVECs cultured in conditioned medium from DDR1-silenced cells was significantly reduced compared to those in control medium. (B) Comparison of gene expression levels of key genes contributing to the angiogenic process in MKN74 control cells and DDR1-silenced cells using qRT-PCR. All results were normalized to levels of the *GAPDH* gene. ($n=3$). Data are expressed as means + SEM.

microvessel area (both Lyve-1 and CD31) of DDR1-silenced tumors was significantly reduced compared with that of MKN74 tumors (Figure 2, *D* and *E*). Ki-67 signals were detected in lymphatic and vascular endothelial cells in control tumors but not in DDR1-silenced tumors. There was no significant difference between the proliferation indexes of the viable regions of MKN74 tumors and DDR1-silenced tumors (Figure 2*F*). These results indicate that DDR1 plays a significant role in the angiogenesis of GC cells *in vitro*.

Table 2. Results of Experimental Liver Metastatic Tumor 6 Weeks after Splenic Implantation

Group	Tumor incidence (spleen)	Liver metastasis		metastasis volume (mm^3)		Number of metastatic foci	
MKN74 scramble (Ctrl) (n=8)	5/5	5/5 (100 %)	*	482.0 (73.5 to 1615.5)	*	12.0 (5 to 19)	*
MKN74 DDR1 shRNA (n=8)	6/6	1/6 (16.7 %)		6.7 (0 to 40.5)		0.5 (0 to 3)	

*P<.05.

Effects of DDR1 Silencing on Angiogenesis

To investigate the effects of DDR1 on angiogenesis, we performed tube formation assays using conditioned media from control and DDR1-silenced MKN74 cells. We found that the mean number of complete tubular structures formed by HUVECs in the conditioned medium from DDR1 control cells was significantly higher than that of DDR1-silenced cell medium (Figure 3*A*). Next, we examined the expression of several angiogenic factors by qRT-PCR of control cells and DDR1-silenced cells. As shown in Figure 3*B*, DDR1 silencing suppressed the expression of key genes associated with angiogenesis. In particular, the expression levels of vascular endothelial growth factor (VEGF)-A, platelet-derived growth factor (PDGF)-B, and VEGF-C were significantly decreased.

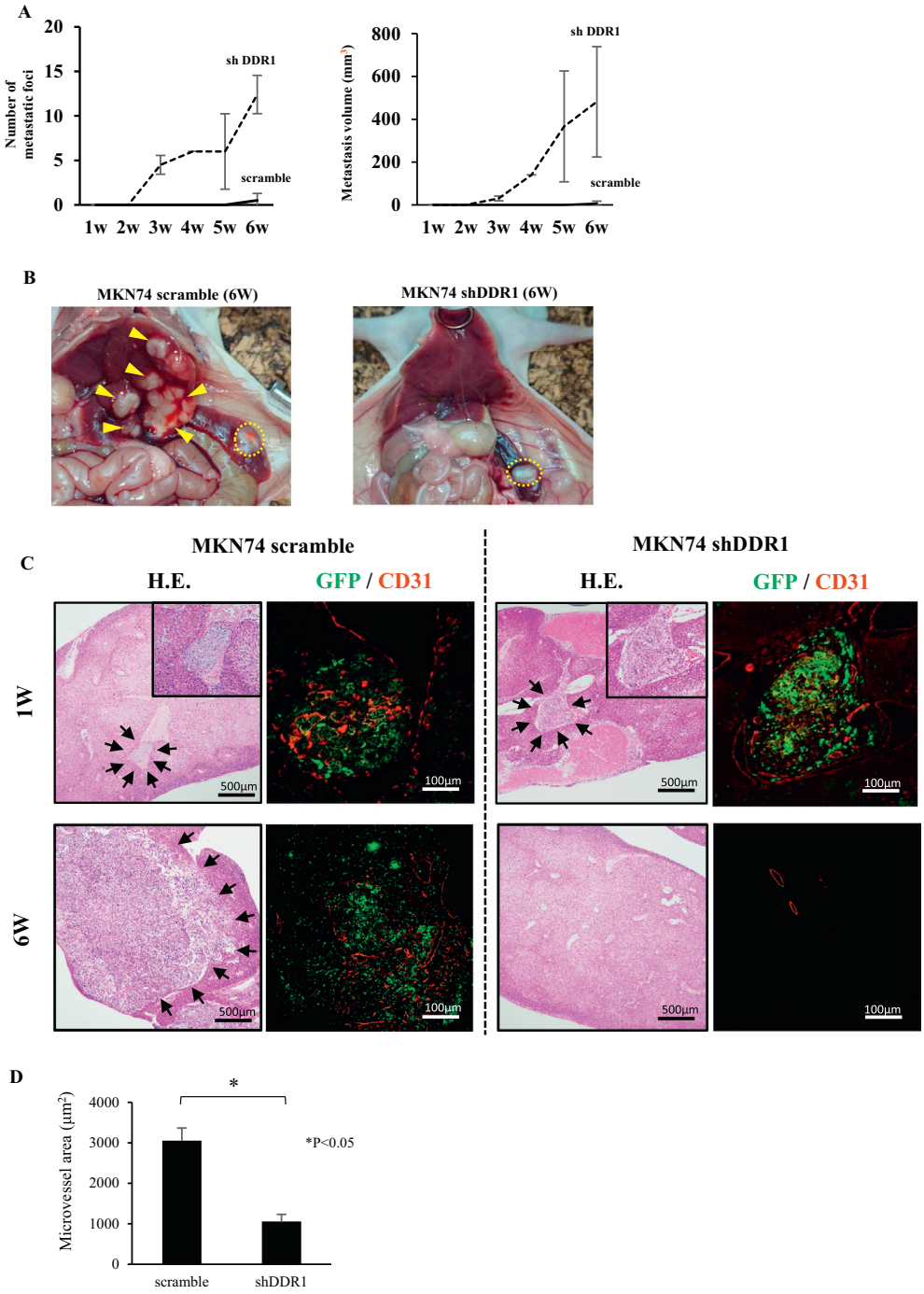

Figure 4. Experimental liver metastatic model using MKN74 cells. (A) Morphological analysis of liver metastatic foci of DDR1-silenced and control MKN74 cells. Left, mean tumor number; right, mean tumor volume. (B) Representative image of implanted splenic tumor and liver metastatic foci at 42 days after implantation. It was visually confirmed that there were many liver metastatic foci in control livers, while in the shDDR1 group, there were no metastatic lesions in the liver in spite of observed splenic engraftment. Yellow circle: primary splenic tumor. Yellow arrow head: liver metastasis. (C) Immunohistochemical analysis of liver metastasis. One week after implantation, micrometastatic lesions were detected by hematoxylin and eosin staining in both control and shDDR1 implanted tumors. Six weeks after implantation, liver metastasis was enlarged in control tumors (black arrow), while no liver metastatic foci were observed in shDDR1 implanted tumors. Several GFP-positive solitary cells were observed in the vessels however. (D) CD31 immunofluorescent staining of micrometastatic foci at 1 week after splenic implantation in each group. Right, mean microvessel area in each group. Microvessel area was significantly reduced in DDR1-silenced micrometastatic foci. Data are expressed as means ± SEM. $^{**}P < .01$.

Effect of DDR1 Silencing in Experimental Liver Metastasis Model

Because DDR1 is involved in the regulation of motility, invasion, and angiogenesis, we hypothesized that DDR1 signaling in GC cells may play an important role in distant metastasis. To investigate the effect of DDR1 on liver metastasis, both MKN74 control cells and shDDR1 cells were implanted into the spleens of nude mice to produce experimental liver metastasis. To detect micrometastasis, cancer cells were labeled with GFP. Mice were sacrificed, and

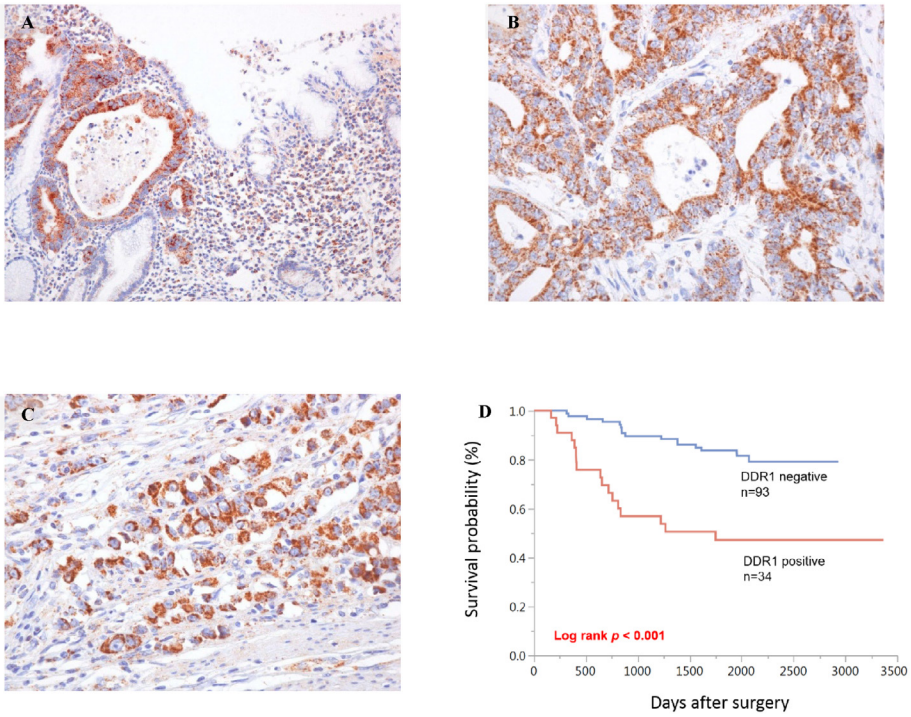

Figure 5. Immunohistochemical analyses of DDR1 in surgical specimens from patients with GC. (A) Representative images of immunohistochemical staining at the border between the normal mucosa (right) and carcinoma (left). (B, C) Representative immunohistochemical staining images of DDR1 in human GC tissue samples. Both intestinal-type (B) and diffuse-type (C) human GC tissues showed immunopositivity in cancer cell membranes and cytoplasms. (D) Kaplan-Meier survival curves showed that overall survival was significantly shorter in the DDR1-positive group than in the negative group ($P < .001$).

histological examinations were performed each week after implantation to detect liver metastases (Table 2). Liver metastasis occurred in 100% of control cells, whereas DDR1-silenced cells did not metastasize. Both the volume and the number of macroscopic liver metastatic foci were dramatically suppressed in DDR1-silenced cells (Figure 4, *A* and *B*). At 2 weeks after implantation, macroscopic liver metastases were not detected in either group (Figure 4*A*). However, we detected microscopic tumor embolisms under the microscope in both groups at 1 and 2 weeks after implantation (Figure 4*C*, *upper panel*). We also observed multiple minute hepatic infarctions in both groups at 1 week after implantation, which we believe were caused by tumor embolisms. At 3 weeks after implantation, liver metastases were enlarged in the control group, while no metastatic foci were detected in the DDR1-silenced group (Figure 4, *A-C*, *lower panel*). We compared the mean microvessel areas of microscopic liver metastatic foci (tumor embolisms) at 1 week after implantation in the two groups. The mean microvessel area was significantly lower in DDR1-silenced foci than in control foci (Figure 4*D*).

Immunohistochemical Analysis of DDR1 in GC Tissues

Finally, we examined the clinicopathological significance of DDR1 through immunohistochemical analysis of 127 GC tissue samples. In normal gastric mucosae, no staining of DDR1 was observed in epithelial cells, whereas some GC tissues showed immunoreactivity in cancer cell membranes and cytoplasms (Figure 5, *A-C*). DDR1 expression was observed in both intestinal-type GC (Figure 5*B*) and diffuse-type GC (Figure 5*C*). In total, 34 (27%) of 127 GC cases were positive for DDR1. We next examined the relationships between DDR1 staining and clinicopathological characteristics (Table 3). Positivity for DDR1 was significantly associated with advanced T grade (depth of invasion; $P < .001$), N grade (degree of lymph node metastasis; $P < .001$), and M grade (degree of distant metastasis; $P < .001$). Moreover, DDR1 staining was observed more frequently in stage III/IV cases (23/46, 50%) than in stage I/II cases (11/81, 14%; $P < .001$), in lymphatic invasion–positive cases (30/68, 44%) than in negative cases (4/59, 7%; $P < .001$), and in vascular invasion–positive cases (23/52, 44%) than in negative cases (11/75, 15%; $P < .001$). However, no correlations with age, sex, or histological classification were observed. Kaplan-Meier analysis showed poorer survival in DDR1-positive GC cases than in DDR1-negative GC cases ($P < .001$, Figure 5*D*). Univariate and multivariate Cox proportional-hazards analyses showed that DDR1 expression was an independent prognostic predictor of survival in patients with GC (Table 4).

Discussion

Tumor cells must undergo a series of sequential, interrelated, selective steps for metastasis to occur. These steps include growth, vascularization, invasion of the host stroma, entrance into and survival in the circulatory system, adhesion to capillary endothelial cells, extravasation into the organ parenchyma, response to local growth factors, proliferation, and induction of vascularization. Tumor growth and metastasis are determined not by cancer cells alone but also by interactions between cancer cells and various kinds of stromal components. The tumor stroma consists of carcinoma-associated fibroblasts, smooth muscle cells, inflammatory cells, microvessels, and abundant ECM [25]. Collagen fibers are the most abundant fibrous protein within the ECM. DDR1 is an RTK that is activated by most

Table 3. Relationship between DDR1 Expression and Clinicopathologic Characteristics

	DDR1 Expression		*P* Value
	Positive	Negative	
Age			
≤65	18 (25%)	53	.684
>65	16 (29%)	40	
Sex			
Male	25 (32%)	53	.090
Female	9 (18%)	40	
T classification			
T1	2 (4%)	53	<.001
T2/3/4	32 (44%)	40	
N classification			
N0	8 (12%)	58	<.001
N1/2/3	26 (43%)	35	
M classification			
M0	15 (15%)	84	<.001
M1	19 (68%)	9	
Stage			
Stage I/II	11 (14%)	70	<.001
Stage III/IV	23 (50%)	23	
ly			
Negative	4 (7%)	55	<.001
Positive	30 (44%)	38	
v			
Negative	11 (15%)	64	<.001
Positive	23 (44%)	29	
Histologic type			
Well	18 (29%)	44	.574
Poorly	16 (25%)	49	

Table 4. Univariate and Multivariate Cox Regression Analysis of DDR1 Expression

	Univariate Analysis		Multivariate Analysis	
	HR (95% CI)	*P* Value	HR (95% CI)	*P* Value
Age (years)		.601		.925
≤65	1 (Ref.)		1 (Ref.)	
>65	1.200 (0.601-2.385)		1.033 (0.513-2.067)	
Sex		.097		.222
Female	1 (Ref.)		1 (Ref.)	
Male	1.865 (0.898-4.241)		1.636 (0.749-3.865)	
Stage		<.001		<.001
I/II	1 (Ref.)		1 (Ref.)	
III/IV	14.635 (6.415-39.442)		11.737 (4.998-32.284)	
Histologic type		.448		.135
Poorly	1 (Ref.)		1 (Ref.)	
Well	1.305 (0.658-2.627)		1.737 (0.840-3.617)	
DDR1		<.001		.049
Negative	1 (Ref.)		1 (Ref.)	
Positive	4.108 (2.059-8.234)		2.066 (1.004-4.281)	

matrix collagens, such as types I to V, VIII, and XI, and it has been shown to be involved in numerous cellular functions, including differentiation, proliferation, adhesion, migration, and invasion [26–30].

Cell migration and invasion are central processes in the development and metastasis of cancer. The regulation of cell migration by DDR1 has been reported in many types of cancer cell lines; however, conflicting results have been reported regarding the inhibitory as well as promotive effects of DDR1 in cell migration [31–34]. Cancer invasion is a process that requires protease-mediated degradation of the stroma and tissue remodeling. Reports from various laboratories using Matrigel as a matrix barrier suggest that DDR1 promotes the invasion of various human cancer cell lines [11,35,36]. We also showed that DDR1 is required for the invasion of GC cells using a Matrigel invasion assay. The upregulation of matrix metalloproteinase (MMP) activity has been reported to accelerate the proinvasive activity of DDR1, and most ECM and basement membrane components can be degraded by MMP-2 and MMP-9 [11,30,36]. Consistent with other reports, DDR1-silenced GC cells exhibited significantly inhibited migration and invasion activities compared to control cells in the present study. In an orthotopic transplantation model, we found that the mean microvascular area was significantly lower in DDR1-silenced tumors than in controls. These findings suggest that DDR1 plays an important role in the angiogenic activity of tumor progression. The majority of the DDR1-silenced tumors consisted of necrotic tissue, and proliferating cells were detected only in the peripheries of the tumors. We speculated that tumor center necrosis was due to the absence of angiogenesis and that the peripheries of tumors were maintained by surrounding normal tissue. In contrast, angiogenic activity was sufficient to maintain control tumors. Little has been reported on the relationship between DDR1 and angiogenesis. Song et al. reported that conditioned medium from DDR1-overexpressing renal cell cancer cells significantly increased the number of tubular structures according to a tube formation assay [37]. Interestingly, DDR1 silencing significantly suppressed the expression of VEGF-A, VEGF-C, and PDGF-B, which are important angiogenic and lymph-angiogenic regulators in GC [38,39]. Therefore, DDR1 silencing seems to concurrently inhibit several steps of the metastasis cascade, such as angiogenesis, migration, and invasion.

Recently, DDR1 has been reported to be capable of inducing multiorgan site metastatic reactivation in breast cancer via noncanonical DDR1 signaling [40]. Consistent with this report, DDR1-silenced GC cells were almost completely suppressed in our liver metastatic model. We found that DDR1-silenced micrometastatic foci did not grow, and the mean microvessel area was significantly reduced compared to that of controls. These results suggest that DDR1 could be used as a novel target for preventing liver metastasis, especially if GC is detected at an early stage of progression.

DDR1 is also known to mediate cell adhesion to collagen. The overexpression of DDR1 promotes cell adhesion to collagen in several cancer cells, such as leukocytes, glioma cells, and pituitary adenoma cells [41,42], whereas DDR1 knockout in smooth muscle cells reduced adhesion to collagen [43]. These findings support the notion that DDR1 expression in cancer cells could facilitate colonization at distant organs during the metastatic process. However, the precise molecular mechanisms underlying these processes are not clearly understood, and further investigation is required.

In our final set of experiments, we examined the role of DDR1 using surgical specimens of human GC tissue. Consistent with our experimental results, the expression of DDR1 was significantly associated with N and M classification and was an independent prognostic classifier of patients with GC. It is noteworthy that prognosis is not related to histological type but rather is dependent on expression of DDR1. Investigating the immunostaining of DDR1 in GC cells may be helpful for determining the therapeutic strategy after surgery.

In conclusion, silencing of the DDR1 gene in GC cells resulted in concurrent inhibition of cell migration, invasion, and angiogenesis, which are sequential, interrelated, selective steps for distant metastasis. We also showed that DDR1 silencing in tumors inhibited metastasis (lymph nodes and liver) in both orthotopic and experimental liver metastatic models. Overall, these results suggest that DDR1 is not only a clinically useful prognostic marker but also a promising molecular target of therapy for GC.

Supplementary data to this article can be found online at https://doi.org/10.1016/j.tranon.2018.02.003.

References

[1] Karimi P, Islami F, Anandasabapathy S, Freedman ND, and Kamangar F (2014). Gastric cancer: descriptive epidemiology, risk factors, screening, and prevention. *Cancer Epidemiol Biomarkers Prev* **23**, 700–713.

[2] Patru CL, Surlin V, Georgescu I, and Patru E (2013). Current issues in gastric cancer epidemiology. *Rev Med Chir Soc Med Nat Iasi* **117**, 199–204.

[3] Liang XJ, Chen C, Zhao Y, and Wang PC (2010). Circumventing tumor resistance to chemotherapy by nanotechnology. *Methods Mol Biol* **596**, 467–488.

[4] Jinawath N, Furukawa Y, Hasegawa S, Li M, Tsunoda T, Satoh S, Yamaguchi T, Imamura H, Inoue M, and Shiozaki H, et al (2004). Comparison of gene-expression profiles between diffuse- and intestinal-type gastric cancers using a genome-wide cDNA microarray. *Oncogene* **23**, 6830–6844.

[5] Vogel W, Gish GD, Alves F, and Pawson T (1997). The discoidin domain receptor tyrosine kinases are activated by collagen. *Mol Cell* **1**, 13–23.

[6] Valiathan RR, Marco M, Leitinger B, Kleer CG, and Fridman R (2012). Discoidin domain receptor tyrosine kinases: new players in cancer progression. *Cancer Metastasis Rev* **31**, 295–321.

[7] Vogel WF, Abdulhussein R, and Ford CE (2006). Sensing extracellular matrix: an update on discoidin domain receptor function. *Cell Signal* **18**, 1108–1116.

[8] Leitinger B and Hohenester E (2007). Mammalian collagen receptors. *Matrix Biol* **26**, 146–155.

[9] Fu HL, Valiathan RR, Arkwright R, Sohail A, Mihai C, Kumarasiri M, Mahasenan KV, Mobashery S, Huang P, and Agarwal G, et al (2013). Discoidin domain receptors: unique receptor tyrosine kinases in collagen-mediated signaling. *J Biol Chem* **288**, 7430–7437.

[10] Alves F, Vogel W, Mossie K, Millauer B, Hofler H, and Ullrich A (1995). Distinct structural characteristics of discoidin I subfamily receptor tyrosine kinases and complementary expression in human cancer. *Oncogene* **10**, 609–618.

[11] Yang SH, Baek HA, Lee HJ, Park HS, Jang KY, Kang MJ, Lee DG, Lee YC, Moon WS, and Chung MJ (2010). Discoidin domain receptor 1 is associated with poor prognosis of non-small cell lung carcinomas. *Oncol Rep* **24**, 311–319.

[12] Quan J, Yahata T, Adachi S, Yoshihara K, and Tanaka K (2011). Identification of receptor tyrosine kinase, discoidin domain receptor 1 (DDR1), as a potential biomarker for serous ovarian cancer. *Int J Mol Sci* **12**, 971–982.

[13] Park HS, Kim KR, Lee HJ, Choi HN, Kim DK, Kim BT, and Moon WS (2007). Overexpression of discoidin domain receptor 1 increases the migration and invasion of hepatocellular carcinoma cells in association with matrix metalloproteinase. *Oncol Rep* **18**, 1435–1441.

[14] Ford CE, Lau SK, Zhu CQ, Andersson T, Tsao MS, and Vogel WF (2007). Expression and mutation analysis of the discoidin domain receptors 1 and 2 in non-small cell lung carcinoma. *Br J Cancer* **96**, 808–814.

[15] Miao L, Zhu S, Wang Y, Li Y, Ding J, Dai J, Cai H, Zhang D, and Song Y (2013). Discoidin domain receptor 1 is associated with poor prognosis of non–small cell lung cancer and promotes cell invasion via epithelial-to-mesenchymal transition. *Med Oncol* **30**, 626.

[16] Huo Y, Yang M, Liu W, Yang J, Fu X, Liu D, Li J, Zhang J, Hua R, and Sun Y (2015). High expression of DDR1 is associated with the poor prognosis in Chinese patients with pancreatic ductal adenocarcinoma. *J Exp Clin Cancer Res* **34**, 88.

[17] Hur H, Ham IH, Lee D, Jin H, Aguilera KY, Oh HJ, Han SU, Kwon JE, Kim YB, and Ding K, et al (2017). Discoidin domain receptor 1 activity drives an aggressive phenotype in gastric carcinoma. *BMC Cancer* **17**, 87.

[18] Shen Q, Cicinnati VR, Zhang X, Iacob S, Weber F, Sotiropoulos GC, Radtke A, Lu M, Paul A, and Gerken G, et al (2010). Role of microRNA-199a-5p and discoidin domain receptor 1 in human hepatocellular carcinoma invasion. *Mol Cancer* **9**, 227.

[19] Ongusaha PP, Kim JI, Fang L, Wong TW, Yancopoulos GD, Aaronson SA, and Lee SW (2003). p53 induction and activation of DDR1 kinase counteract p53-mediated apoptosis and influence p53 regulation through a positive feedback loop. *EMBO J* **22**, 1289–1301.

[20] Medici D and Nawshad A (2010). Type I collagen promotes epithelial-mesenchymal transition through ILK-dependent activation of NF-kappaB and LEF-1. *Matrix Biol* **29**, 161–165.

[21] Oue N, Motoshita J, Yokozaki H, Hayashi K, Tahara E, Taniyama K, Matsusaki K, and Yasui W (2002). Distinct promoter hypermethylation of p16INK4a, CDH1, and RAR-beta in intestinal, diffuse-adherent, and diffuse-scattered type gastric carcinomas. *J Pathol* **198**, 55–59.

[22] Lauren P (1965). The two histological main types of gastric carcinoma: diffuse and so-called intestinal-type carcinoma. An attempt at a histo-clinical classification. *Acta Pathol Microbiol Scand* **64**, 31–49.

[23] Sumida T, Kitadai Y, Shinagawa K, Tanaka M, Kodama M, Ohnishi M, Ohara E, Tanaka S, Yasui W, and Chayama K (2011). Anti-stromal therapy with imatinib inhibits growth and metastasis of gastric carcinoma in an orthotopic nude mouse model. *Int J Cancer* **128**, 2050–2062.

[24] Yamazaki K, Onouchi Y, Takazoe M, Kubo M, Nakamura Y, and Hata A (2007). Association analysis of genetic variants in IL23R, ATG16L1 and 5p13.1 loci with Crohn's disease in Japanese patients. *J Hum Genet* **52**, 575–583.

[25] Hanahan D and Weinberg RA (2000). The hallmarks of cancer. *Cell* **100**, 57–70.

[26] Vogel W, Brakebusch C, Fassler R, Alves F, Ruggiero F, and Pawson T (2000). Discoidin domain receptor 1 is activated independently of beta(1) integrin. *J Biol Chem* **275**, 5779–5784.

[27] Roberts ME, Magowan L, Hall IP, and Johnson SR (2011). Discoidin domain receptor 1 regulates bronchial epithelial repair and matrix metalloproteinase production. *Eur Respir J* **37**, 1482–1493.

[28] Curat CA and Vogel WF (2002). Discoidin domain receptor 1 controls growth and adhesion of mesangial cells. *J Am Soc Nephrol* **13**, 2648–2656.

[29] Hachehouche LN, Chetoui N, and Aoudjit F (2010). Implication of discoidin domain receptor 1 in T cell migration in three-dimensional collagen. *Mol Immunol* **47**, 1866–1869.

[30] Ram R, Lorente G, Nikolich K, Urfer R, Foehr E, and Nagavarapu U (2006). Discoidin domain receptor-1a (DDR1a) promotes glioma cell invasion and adhesion in association with matrix metalloproteinase-2. *J Neuro-Oncol* **76**, 239–248.

[31] Hansen C, Greengard P, Nairn AC, Andersson T, and Vogel WF (2006). Phosphorylation of DARPP-32 regulates breast cancer cell migration downstream of the receptor tyrosine kinase DDR1. *Exp Cell Res* **312**, 4011–4018.

[32] Koh M, Woo Y, Valiathan RR, Jung HY, Park SY, Kim YN, Kim HR, Fridman R, and Moon A (2015). Discoidin domain receptor 1 is a novel transcriptional target of ZEB1 in breast epithelial cells undergoing H-Ras-induced epithelial to mesenchymal transition. *Int J Cancer* **136**, E508-520.

[33] Rudra-Ganguly N, Lowe C, Mattie M, Chang MS, Satpayev D, Verlinsky A, An Z, Hu L, Yang P, and Challita-Eid P, et al (2014). Discoidin domain receptor 1 contributes to tumorigenesis through modulation of TGFBI expression. *PLoS One* **9**e111515.

[34] Hu Y, Liu J, Jiang B, Chen J, Fu Z, Bai F, Jiang J, and Tang Z (2014). MiR-199a-5p loss up-regulated DDR1 aggravated colorectal cancer by activating epithelial-to-mesenchymal transition related signaling. *Dig Dis Sci* **59**, 2163–2172.

[35] Shimada K, Nakamura M, Ishida E, Higuchi T, Yamamoto H, Tsujikawa K, and Konishi N (2008). Prostate cancer antigen-1 contributes to cell survival and invasion though discoidin receptor 1 in human prostate cancer. *Cancer Sci* **99**, 39–45.

[36] Castro-Sanchez L, Soto-Guzman A, Guaderrama-Diaz M, Cortes-Reynosa P, and Salazar EP (2011). Role of DDR1 in the gelatinases secretion induced by native type IV collagen in MDA-MB-231 breast cancer cells. *Clin Exp Metastasis* **28**, 463–477.

[37] Song J, Chen X, Bai J, Liu Q, Li H, Xie J, Jing H, and Zheng J (2016). Discoidin domain receptor 1 (DDR1), a promising biomarker, induces epithelial to mesenchymal transition in renal cancer cells. *Tumour Biol* **37**, 11509–11521.

[38] Cao R, Bjorndahl MA, Religa P, Clasper S, Garvin S, Galter D, Meister B, Ikomi F, Tritsaris K, and Dissing S, et al (2004). PDGF-BB induces intratumoral lymphangiogenesis and promotes lymphatic metastasis. *Cancer Cell* **6**, 333–345.

[39] Onoyama M, Kitadai Y, Tanaka Y, Yuge R, Shinagawa K, Tanaka S, Yasui W, and Chayama K (2013). Combining molecular targeted drugs to inhibit both cancer cells and activated stromal cells in gastric cancer. *Neoplasia* **15**, 1391–1399.

[40] Gao H, Chakraborty G, Zhang Z, Akalay I, Gadiya M, Gao Y, Sinha S, Hu J, Jiang C, and Akram M, et al (2016). Multi-organ site metastatic reactivation mediated by non-canonical discoidin domain receptor 1 signaling. *Cell* **166**, 47–62.

[41] Kamohara H, Yamashiro S, Galligan C, and Yoshimura T (2001). Discoidin domain receptor 1 isoform-a (DDR1alpha) promotes migration of leukocytes in three-dimensional collagen lattices. *FASEB J* **15**, 2724–2726.

[42] Yoshida D and Teramoto A (2007). Enhancement of pituitary adenoma cell invasion and adhesion is mediated by discoidin domain receptor-1. *J Neuro-Oncol* **82**, 29–40.

[43] Hou G, Vogel W, and Bendeck MP (2001). The discoidin domain receptor tyrosine kinase DDR1 in arterial wound repair. *J Clin Invest* **107**, 727–735.